Methylammonium Lead Bromide Perovskite Light Emitting Diodes by Chemical Vapor Deposition

*Matthew R. Leyden,[1]† Lingqiang Meng,[1]†, Yan Jiang,[1], Luis K. Ono[1], Longbin Qiu,[1] Emilio J. Juarez-Perez,[1]Chuanjiang Qin,[2] Chihaya Adachi,[2] and Yabing Qi [1]**

[1] Energy Materials and Surface Sciences Unit (EMSS), Okinawa Institute of Science and Technology Graduate University (OIST), 1919-1 Tancha, Onna-son, Kunigami-gun, Okinawa 904-0495, Japan

[2] Center for Organic Photonics and Electronics Research (OPERA), Kyushu University, 744 Motooka, Nishi-ku, Fukuoka 819-0395, Japan

AUTHOR INFORMATION

†These authors contributed equally to this work.

*Corresponding Author: Yabing Qi, email: Yabing.Qi@OIST.jp

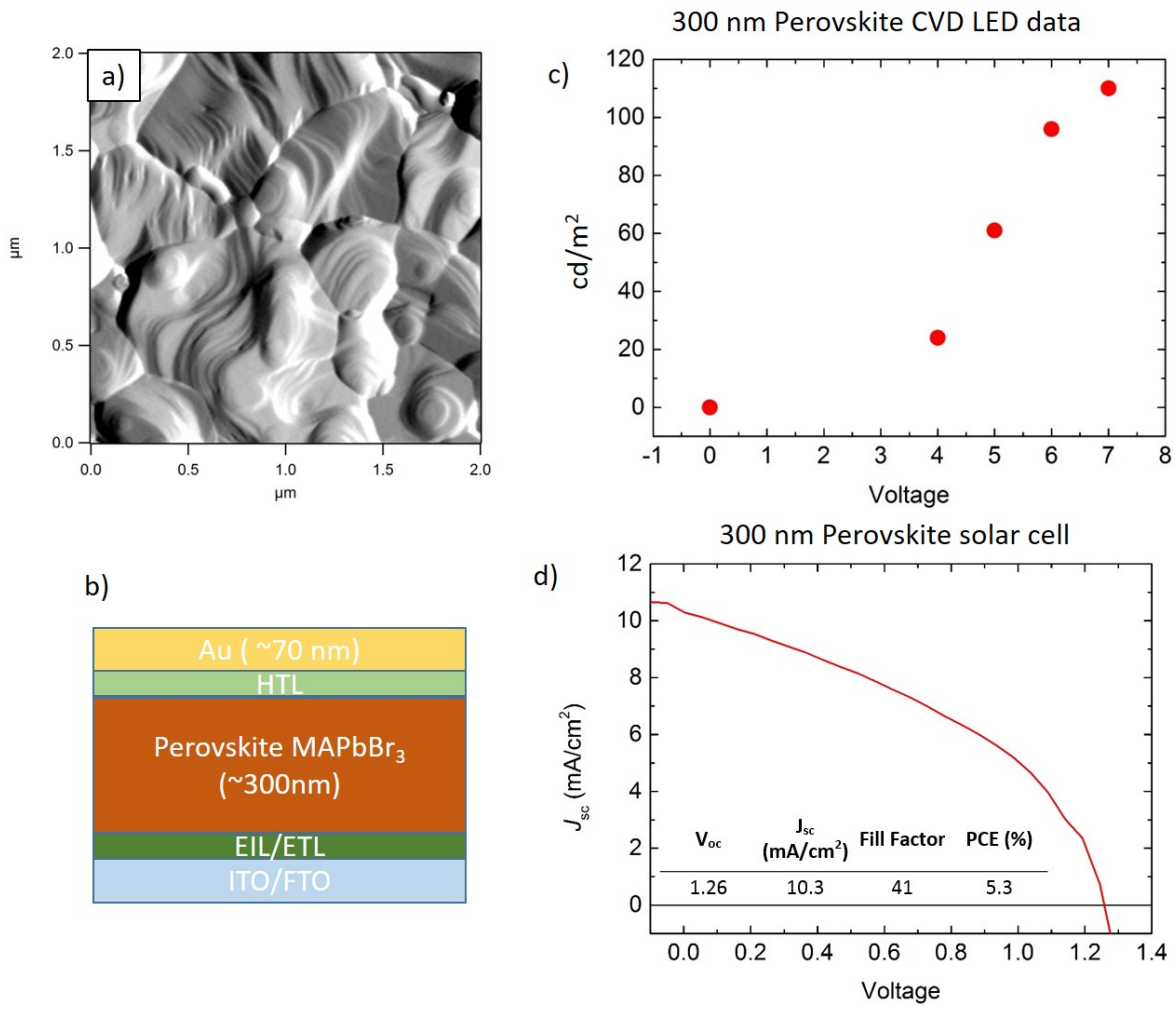

Figure S1. 300 nm thick films of $MAPbBr_3$. A) Atomic force microscope amplitude image of $MAPbBr_3$ film showing laminate structure. B) Device geometry, for solar cells the electron transport layer (ETL) was spray coated TiO_2, and the hole transport layer P3HT. For LEDs, the electron injection layer (EIL) was PFN-OX, and the hole transport layers (HTL) were TAPC and MoO_3. C) LED luminance data collected from 300 nm thick perovskite LEDs. D) Champion solar cell using a CVD grown $MAPBBr_3$ film.

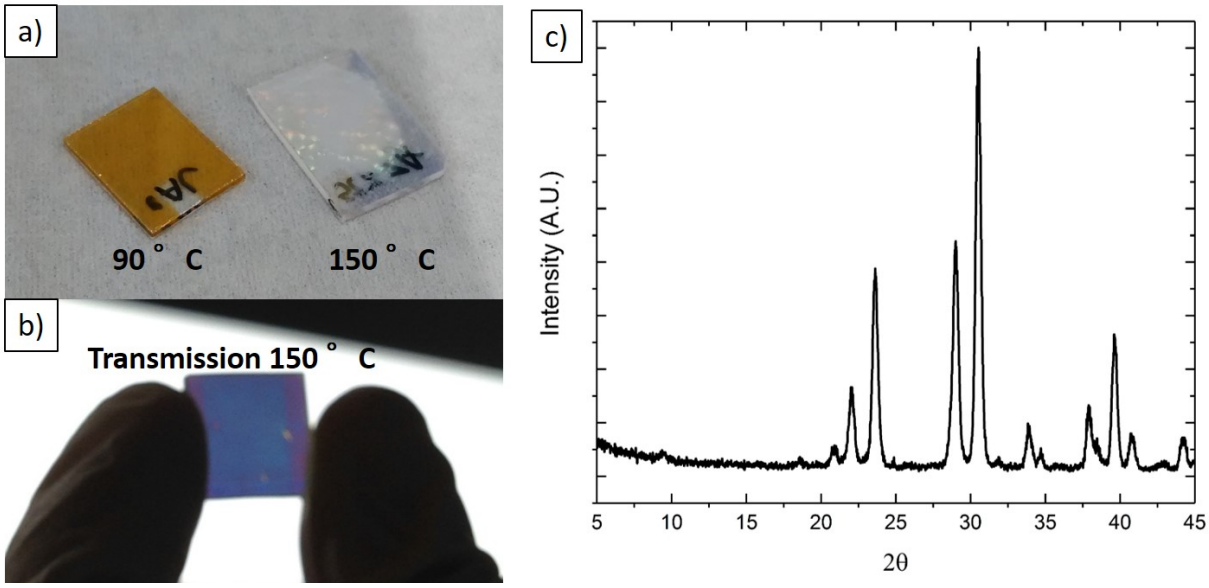

Figure S2. Films grown at high temperature will not convert to perovskite. a) Image of films after growth with substrate temperature of 90 °C and 150 °C. b) Film grown at 150 °C seen in transmission c) XRD spectrum of the film grown at 150 °C. No perovskite peak was measured in the XRD spectra, only $PbBr_2$ was apparent. The iridescent appearance and blue color in transmission were likely due to $PbBr_2$ crystal growth, surface roughening, and possible adsorbed but unreacted MABr on the top surface. Growths done at temperatures above 120 °C were not stable. With a high deposition rate of MABr, it was possible to convert the film to perovskite for a short time, but if the rate decreased the resultant film would be like that shown on the right of S2a.

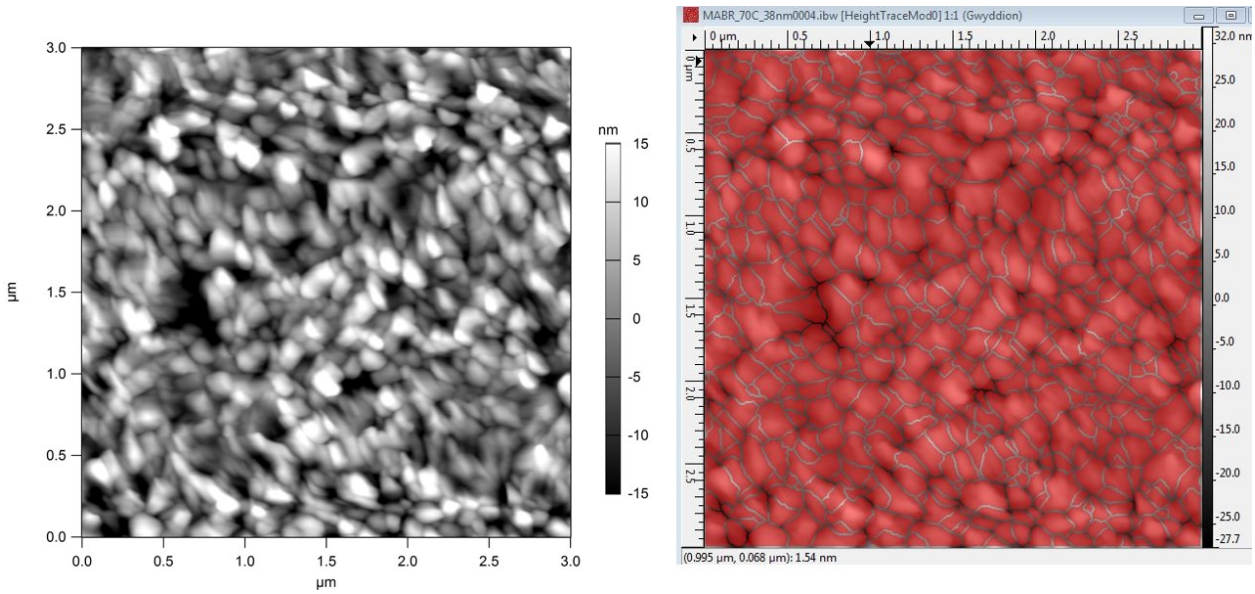

Figure S3. Grain size calculation was performed using Gwyddion watershed technique on AFM height images. We found the following parameters gave approximate visual agreement between apparent grain boundaries and those define by Gwydion. Grain location: 100 steps, 0.1 % drop size, 2 px^2 threshold, segmentation 1000 steps, 100% threshold.

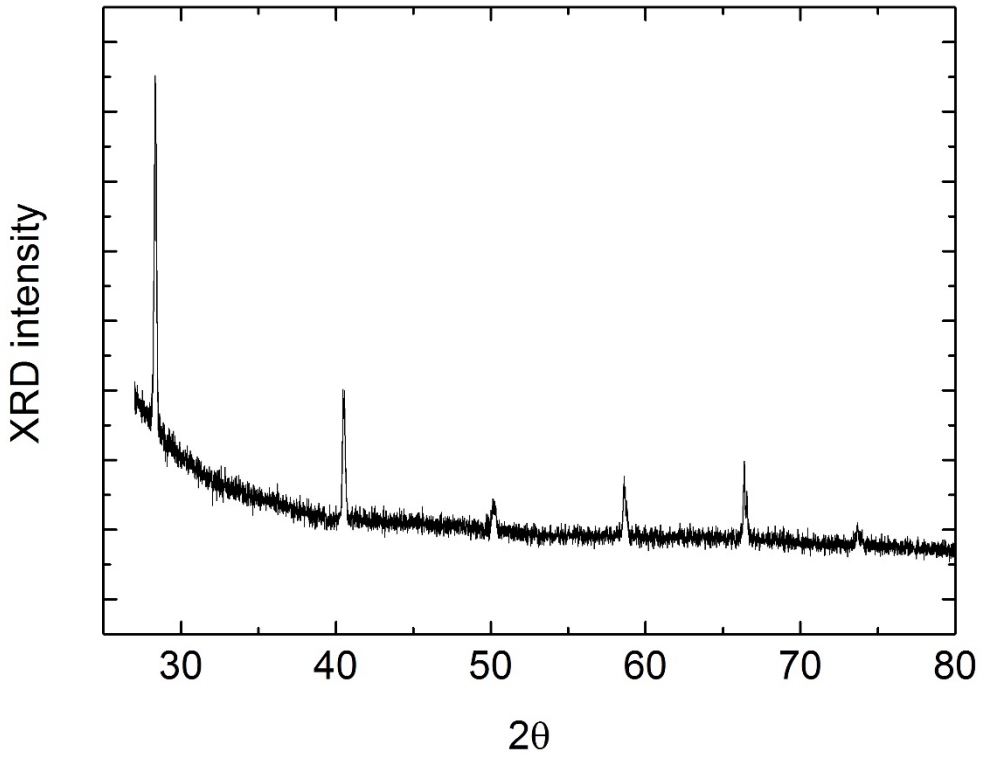

Figure S4. XRD spectrum of KCl powder used as a highly crystalline reference to determine instrument broadening. Ideally, we should measure broadening as a function of angle, however no significant peak of our reference aligned with the primary (100) peak of $MAPbBr_3$. Alternatively we measured the average FWHM of all peaks to be 0.12^o +/- 0.04. The crystal size measurement depends significantly on this broadening measurement, so given the large error we could not come to a strong conclusion about the exact size or ratio of crystal size. Given the error in the broadening measurement the ratio in crystal size of 120 °C / 90 °C growth can range from 2:1 to 5:1.

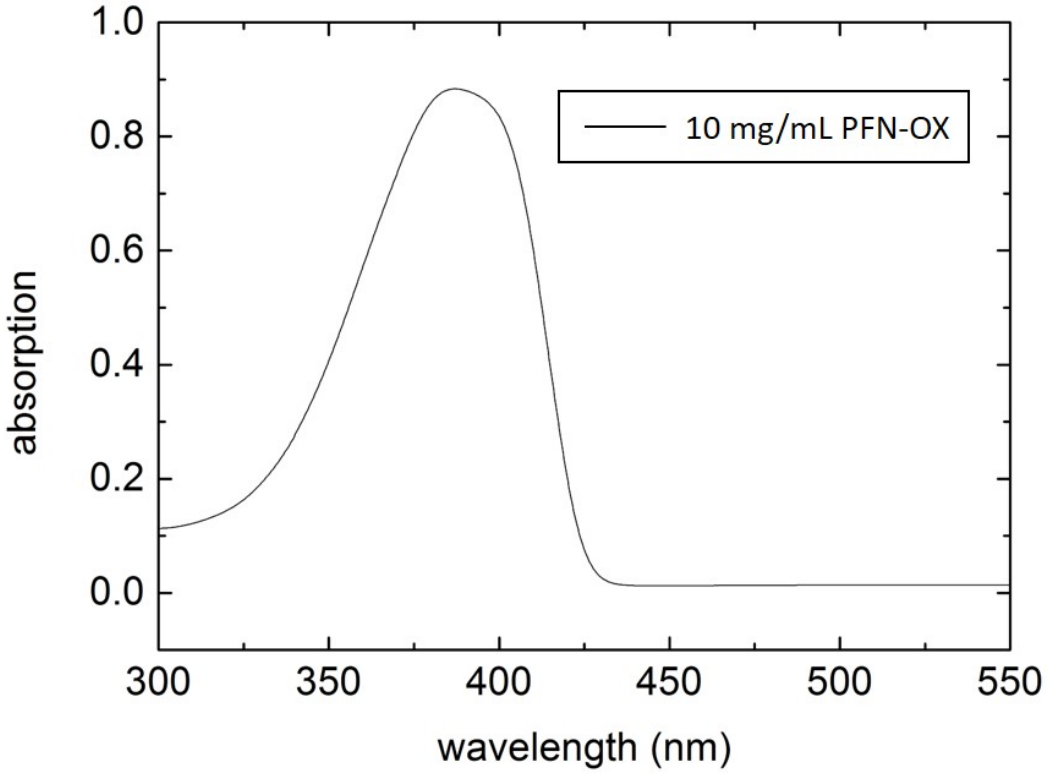

Figure S5. Absorption spectra of PFN on glass. A solution of 10 mg/mL PFN in methanol was spun onto a glass substrate. The absorption edge was at ~430 nm (2.88 eV). Given a work function of 3.55 and HOMO level of 5.38, this would give a LUMO level of 2.50 eV. See Fig. S6.

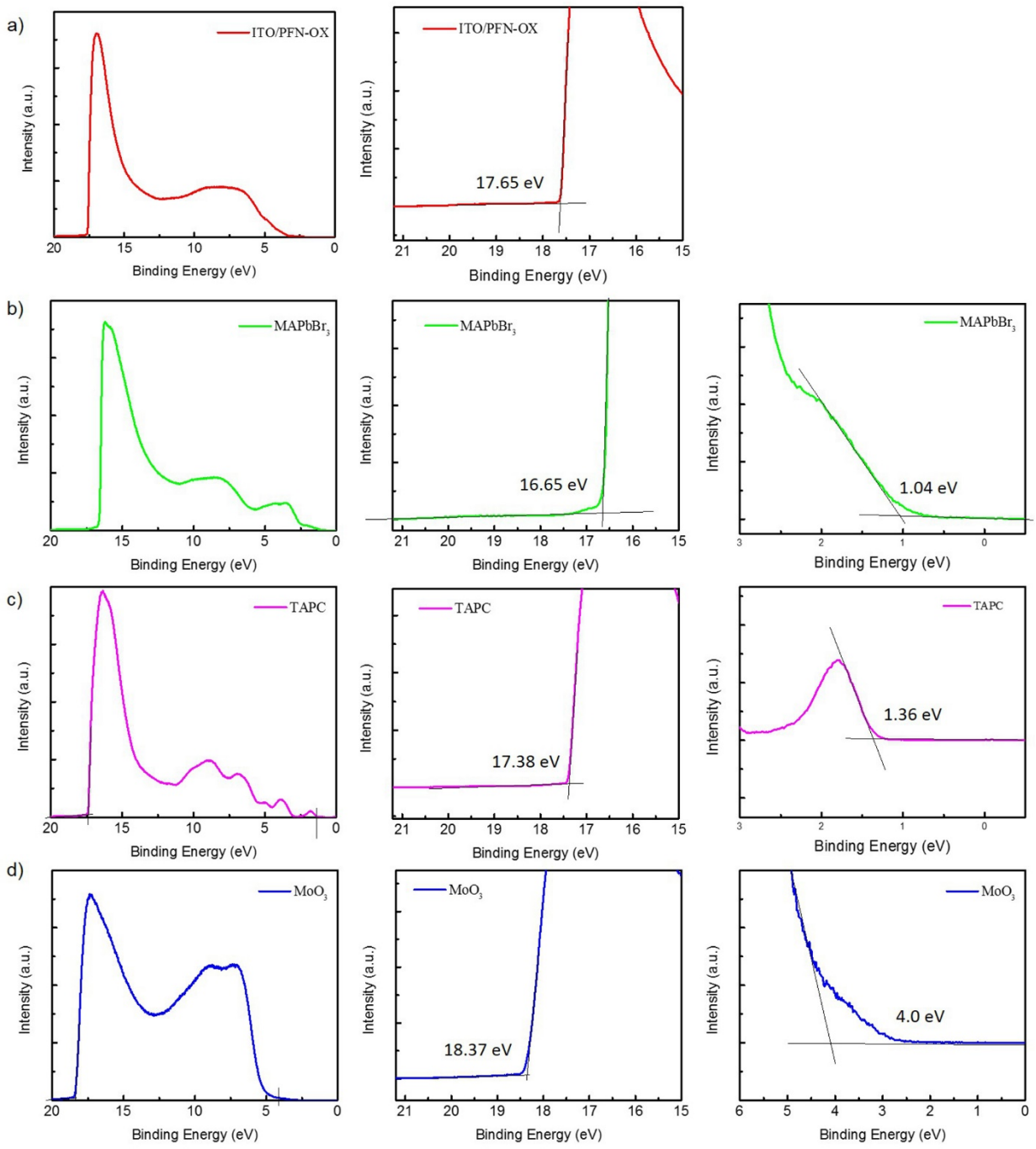

Figure S6. Detailed UPS spectra for a) ITO/PFN-OX, b) ITO/PFN-OX/$MAPbBr_3$, c) ITO/PFN-OX/$MAPbBr_3$/TAPC, d) ITO/PFN-OX/$MAPbBr_3$/TAPC/MoO_3. The plotted curves are the average of 5 scans. The fitting for MoO_3 was not well defined but represents a best guess.

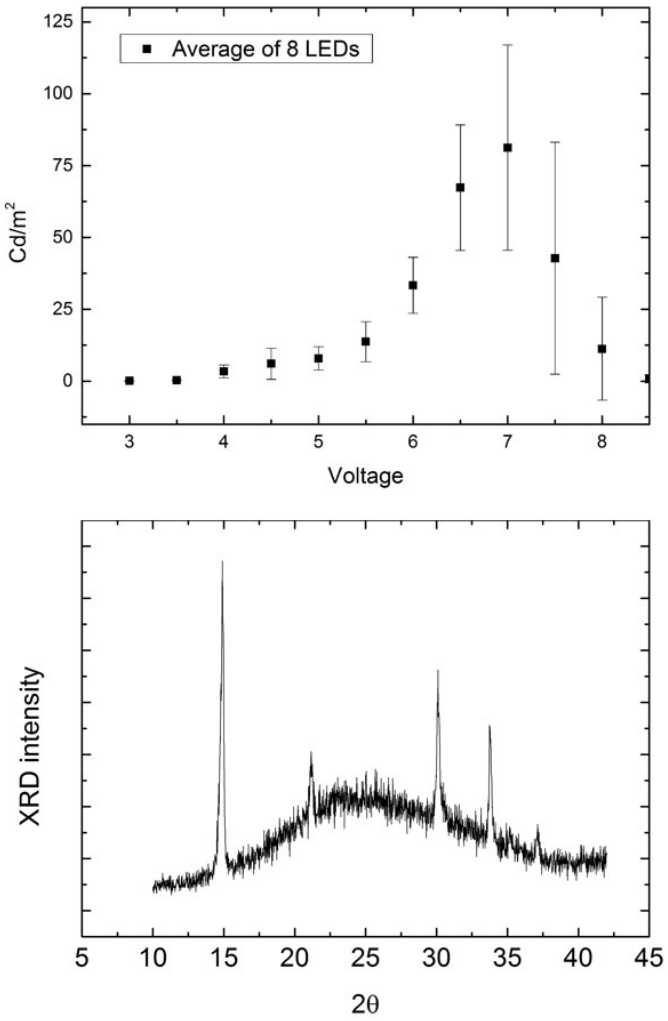

Figure S7. Performance of CVD perovskite LEDs grown at 70 °C. The second graph shows an XRD spectrum of a 70 °C grown film. The full width half maximum of this sample was 0.23°, which is narrower than the example presented in figure 2 grown at 90 °C, suggesting higher or comparable crystallinity. AFM measurements suggest smaller crystal size with decreasing growth temperature. We expected that this would also be expressed in the XRD scans. There may be process variability not expressed in the single set of XRD scans. Unfortunately, the number of XRD measurements was insufficient to make strong conclusions about the average crystallinity.

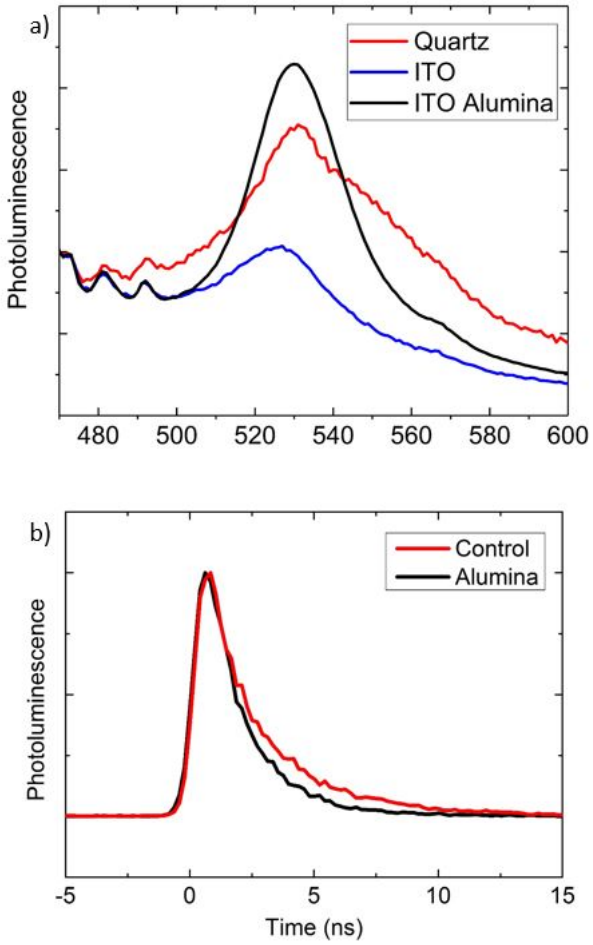

Figure S8. Impact of alumina scaffold on photoluminescence. a) Photoluminescence of a 100 nm thick $MAPbBr_3$ film on a quartz substrate, ITO substrate, and an ITO substrate with an alumina scaffold grown side by side in a CVD growth. The ITO sample with the alumina scaffold had brighter photoluminescence than either the quartz or ITO substrate. This confirms that alumina will act as a scaffold that promotes the growth of small grain perovskite and increase PL, as well as isolate the perovskite from a surface that may quench PL. b) Time resolved photoluminescence measurement (TRPL). Decay lifetimes (1/e) are ~ 2.4 ns. No significant difference was observed between samples with an alumina matrix and those without. TRPL of $MAPbBr_3$ films were measured on ITO/PFN-OX substrates.

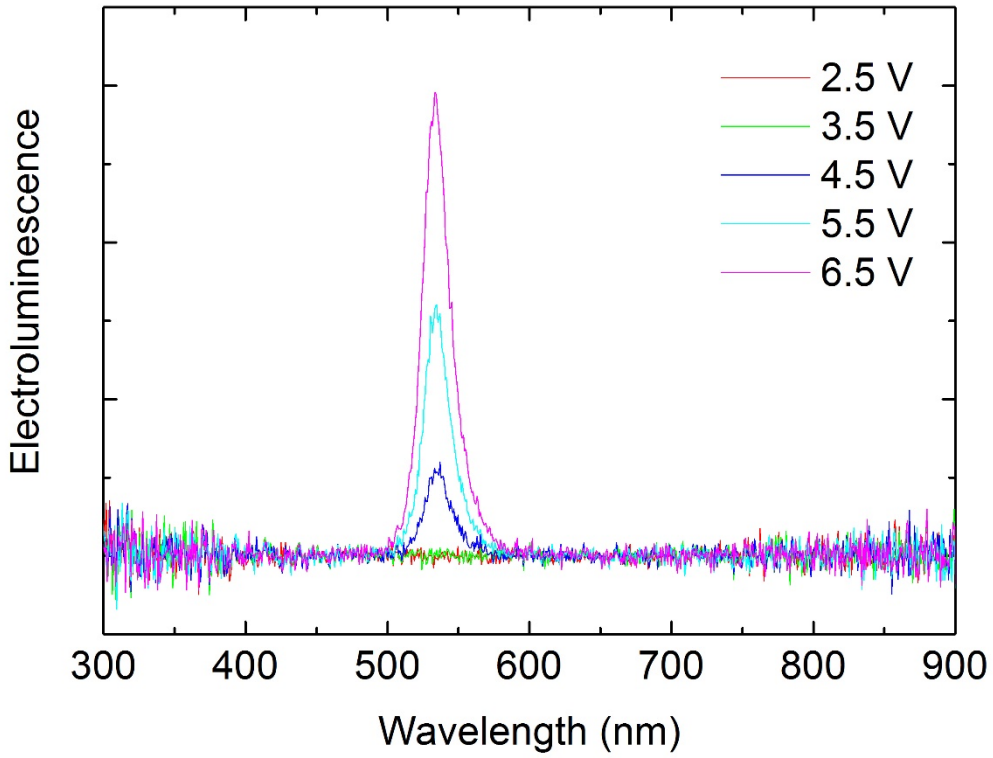

Figure S9. CVD grown perovskite LED using the structure PFN-OX/$MAPbBr_3$/TPT1/MoO_3/Au. This figure only shows emission from the perovskite and not the broadband emission seen in Fig. 5a. This suggests that TAPC was the source of the broad band emission.

Figure S10. Large area CVD perovskite LED operated at 5 V.

Methods

Film Characterization. X-ray diffraction spectra were measured using a Bruker D8 Discover. Atomic Force Microscopy images were taken using an Asylum MFP-3D in AC mode. UV-vis absorbance spectra were measured on a Jasco V-670 spectrometer. Ultra-violet photoelectron spectroscopy was performed with a Kratos Analytical AXIS Ultra DLD (He–Iα = 21.22 eV). Binding energy (BE) for UPS was calibrated by measuring the Fermi edge (EF = 0 eV) on a clean Au surface. Estimated energy resolutions of UPS was 0.15 eV. UV induced sample damage was monitored by taking five consecutive spectra and by comparing those spectra. The time acquisition for each scan was ~15 s. The five scans were averaged to a single spectrum if no changes were observed among them. Photoluminescence measurements were performed on $MAPbBr_3$ films using a 400 nm laser (Spectra-Physics, MAITAI XF-IMW). Time-resolved photoluminescence was acquired using the time-correlated, single-photon counting technique (Hamamatsu, C10627). Excitation was provided by a femtosecond mode-locked Ti:Sapp laser (Spectra-Physics, MAITAI XF-IMW) at 400 nm with an average power at 8 MHz of 0.73 mW.

Perovskite LED Fabrication. LEDs were fabricated on clean ITO glass substrates (10 Ω/□). The ITO substrates were cleaned sequentially in solutions of SDS, water, acetone, and IPA in an ultrasonic cleaner, and then dried on a hotplate at 120 °C. Then a PFN-OX (Lumtec) solution (2 mg/mL, in a solution of 1% acetic acid in methanol) was spin cast onto substrates with a speed of 2500 rpm for 45 seconds, and then annealed in ambient conditions at 120 °C for 20 min. Substrates using alumina were spin coated with a dilute solution of nanoparticles (Sigma Aldrich, suspension < 50 nm) to form approximately 1 monolayer of particles, which were measured to be ~50 nm by a Bruker profilometer. Samples were then loaded into an evaporator for lead bromide (Sigma

Aldrich >98%) deposition at pressures < $2x10^{-3}$ Pa with a rate of ~1 Å/s. Substrates were then transferred into one zone of a 2-zone CVD furnace, and the other zone was loaded with ~50 mg of MABr powder (Dyesol). The CVD furnace was evacuated and purged with nitrogen (~50 sccm, 100 Pa) and then ramped up to temperature. At optimized conditions the substrate zone was held at 90 °C and the MABr zone was held at 150 °C for 45 min. After the CVD process, TAPC (Jilin Optical and Electronic materials) and MoO_3 were deposited by thermal evaporation in succession at ~1 Å/s and ~0.2 Å/s respectively at pressures < $2x10^{-3}$ Pa. Substrates were then transferred to another evaporator for gold deposition (~0.3 Å/s, at < $2x10^{-3}$ Pa).

LED Testing. Current–voltage–brightness characteristics were measured using a Keithley source meter (Keithley 2400) and a Konica Minolta CS-2000 spectroradiometer. EQEs were calculated from the luminance, current density, and EL spectrum, assuming a Lambertian distribution. All the measurements were carried out in ambient atmosphere.